The EMBO Journal vol.13 no.22 pp.5504–5515, 1994

The influenza virus hemagglutinin cytoplasmic tail is not essential for virus assembly or infectivity

Hong Jin[1], George P.Leser[2] and Robert A.Lamb[1,2,3]

[1]Howard Hughes Medical Institute and [2] Department of Biochemistry, Molecular Biology and Cell Biology, Northwestern University, Evanston, IL 60208-3500, USA
[3]Corresponding author

Communicated by K.Simons

The influenza A virus hemagglutinin (HA) glycoprotein contains a cytoplasmic tail which consists of 10–11 amino acids, of which five residues are conserved in all subtypes of influenza A virus. As the cytoplasmic tail is not needed for intracellular transport to the plasma membrane, it has become virtually dogma that the role of the cytoplasmic tail is in forming protein–protein interactions necessary for creating an infectious budding virus. To investigate the role of the HA cytoplasmic tail in virus replication, reverse genetics was used to obtain an influenza virus that lacked an HA cytoplasmic tail. The rescued virus contained the HA of subtype A/Udorn/72 in a helper virus (subtype A/WSN/33) background. Biochemical analysis indicated that only the introduced tail$^-$ HA was incorporated into virions and these particles lacked a detectable fragment of the helper virus HA. The tail$^-$ HA rescued virus assembled and replicated almost as efficiently as virions containing wild-type HA, suggesting that the cytoplasmic tail is not essential for the virus assembly process. Nonetheless, a revertant virus was isolated, suggesting that possession of a cytoplasmic tail does confer an advantage.

Key words: cytoplasmic tail/hemagglutinin/infectivity/influenza virus/virus assembly

Introduction

Many enveloped viruses mature by budding at the plasma membrane of infected cells. In the budding process viral proteins are preferentially incorporated into nascent virions, whereas the majority of host proteins are excluded from the assembly site. It has become virtually dogma that the interaction of viral glycoprotein cytoplasmic tails with viral matrix proteins and nucleocapsids on the cytoplasmic side of the plasma membrane triggers the formation of an infectious budding particle (reviewed in Compans and Choppin, 1975; Simons and Garoff, 1980; Dubois-Dalcq *et al.*, 1984). Although a great deal is known about the structure and functions of the extracellular domains of several viral integral membrane glycoproteins, much less is known about the roles of their transmembrane domains and cytoplasmic tails as definitive data have been difficult to obtain. For the alphaviruses, an interaction between nucleocapsid and the glycoprotein cytoplasmic tail is thought to occur based on both molecular genetic data (Lopez *et al.*, 1994) and on the observation that alterations to the Sindbis virus E2 glycoprotein cytoplasmic tail can abolish virus production (Gaedigk-Nitschko and Schlesinger, 1991). For vesicular stomatitis virus (VSV), based on work done with a ts mutant (tsO45) in which the G glycoprotein is blocked in intracellular transport at the non-permissive temperature, it was originally thought that the G protein is not required for virus assembly. However, subsequent work indicated that the spikeless tsO45 virions grown at the non-permissive temperature contained the C-terminal fragment of G protein including the cytoplasmic domain (Metsikko and Simons, 1986), suggesting an essential role for this domain in viral assembly. More recently it has been found, by using a complementation assay, that at least a portion of the cytoplasmic tail of VSV G protein is required for the G protein to be incorporated into virions and thus for the virus to be infectious (Whitt *et al.*, 1989). The cytoplasmic domain of simian immunodeficiency virus gp160 env modulates virus infectivity (Chakrabarti *et al.*, 1989), but for Rous sarcoma virus (RSV), infectious virions are released from cells infected with proviruses carrying a glycoprotein (gp37) lacking its cytoplasmic domain (Perez *et al.*, 1987). Thus, the cytoplasmic tail of gp37 of RSV is not absolutely required for the assembly process.

The influenza A virus envelope contains two major glycoproteins, neuraminidase (NA) and hemagglutinin (HA) (reviewed in Lamb, 1989) and, in much less abundance, a small integral membrane protein M_2 (Lamb *et al.*, 1985), which has an ion-channel activity (Pinto *et al.*, 1992; Wang *et al.*, 1993). The role of these integral membrane proteins in the assembly process has not been defined. NA is considered to be of limited importance in viral entry into cells, although NA activity is thought to be necessary to release fully formed virions from the infected cell surface (Palese *et al.*, 1974). However, influenza virus mutants of NA, in which NA is blocked in intracellular transport at the non-permissive temperature, do form virus particles at the non-permissive temperature (Palese *et al.*, 1974). However, virions lacking a NA protein may contain the transmembrane domain and cytoplasmic tail of NA. Liu and Air (1993) have described a NA-minus mutant of influenza virus that was produced by addition of exogenous neuraminidase to infected cell cultures and selection with anti-NA antibodies. This NA-minus virus contains an internally deleted NA RNA segment which has the potential to code for the transmembrane domain and cytoplasmic tail of NA (G.Air, personal communication). Thus, this NA domain could remain to be an organizer for viral assembly. HA is essential for virus infectivity because it has receptor-binding activity (Hirst, 1942; Weis *et al.*, 1988) and mediates fusion of the viral envelope with the endosomal

membrane (reviewed in Marsh and Helenius, 1989). However, the available data indicate that HA is not required for assembly of the virion. A temperature-sensitive mutant of HA (A/WSN/33 ts 61S), in which the HA fails to be transported to the cell surface at the non-permissive temperature, forms virions at the non-permissive temperature with high efficiency (Pattnaik *et al.*, 1986). However, these latter data could not exclude the possibility that the HA deficient virus particles contained the HA transmembrane domain and cytoplasmic tail, as was found with the VSV G glycoprotein of the tsO45 virus as discussed above.

The cytoplasmic tail of influenza virus HA has been defined as containing 10–11 amino acids, based on the principle that the charged residue adjacent to the hydrophobic transmembrane domain delineates the boundary of the domain. Analysis of HA sequences of 14 subtypes of influenza viruses showed remarkable conservation in their tail domain (Nobusawa *et al.*, 1991; Simpson and Lamb, 1992). Two conserved cysteine residues in the cytoplasmic tail and one in the transmembrane domain are post-translationally modified by the covalent linkage of palmitate through a thio-ether linkage (Naeve and Williams, 1990; Steinhauer *et al.*, 1991; Viet *et al.*, 1991; Naim *et al.*, 1992). An essential role of palmitoylation for HA fusion activity has been proposed (Naeve and Williams, 1990), but other data do not support this view (Steinhauer *et al.*, 1991; Viet *et al.*, 1991; Naim *et al.*, 1992). Deletion of the cytoplasmic tail of HA does not drastically affect the transport of HA to the cell surface and does not affect the activity of HA in *in vitro* hemadsorption and fusion assays (Doyle *et al.*, 1985, 1986; Simpson and Lamb, 1992). The lack of an essential role of the HA cytoplasmic tail in intracellular transport, and the conservation of sequence in this domain, led to the suggestion that the HA cytoplasmic tail might have a role in virus assembly (Doyle *et al.*, 1985). In support of this view was the finding that a synthetic peptide which mimics the influenza virus A/WSN/33 cytoplasmic tail, when added to infected cells, inhibited the release of infectious virus (Collier *et al.*, 1991). The reverse genetics system for influenza virus developed by Luytjes *et al.* (1989) has made it possible to introduce a cDNA-derived RNA gene segment into an infectious influenza virus genome to study properties of the altered virus. Using this technique, we have investigated further the necessity of the HA cytoplasmic tail for virus assembly and infectivity. We report here studies on the properties of an influenza virus which contains an HA which lacks its cytoplasmic domain.

Results

Generation of transfectant virus containing an HA that lacks a cytoplasmic tail

To generate a rescued (transfectant) influenza virus that contains an HA with an altered cytoplasmic tail, two plasmids were constructed: pT7HA and pT7HAtail$^-$. In using the reverse genetics system, the general principles established by Parvin *et al.* (1989), Luytjes *et al.* (1989) and Enami and Palese (1991) were adopted. pT7HA contained the cDNA for the influenza virus A/Udorn/72 HA. pT7HAtail$^-$ was identical to pT7HA except that a translational stop codon was introduced into HA to replace

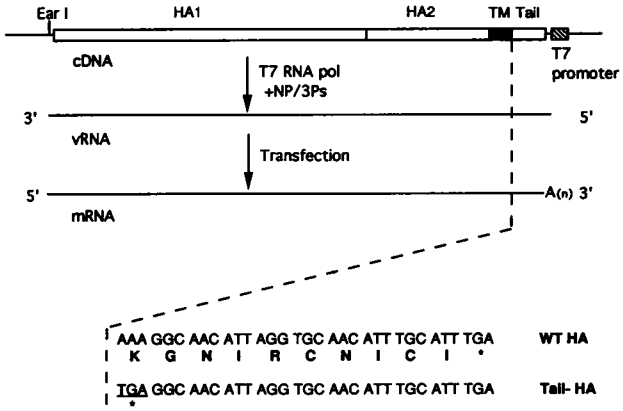

Fig. 1. Schematic diagram of HA and tail$^-$ HA. The expanded region shows the amino acid sequence of wild-type HA cytoplasmic tail, and the nucleotide sequences of the wild-type HA and tail$^-$ HA cDNAs. The cytoplasmic tail of the tail$^-$ HA was deleted by insertion of a translational stop codon. The T7 promoter and the *Ear*I site to linearize the plasmids for synthesizing vRNA are indicated.

the lysine residue at the junction of the transmembrane domain and the cytoplasmic tail (Figure 1).

HA–RNP complexes were reconstituted *in vitro* and transfected into influenza virus A/WSN/33-infected MDBK cells. To select for rescued virus containing A/Udorn HA, cultures were incubated with a pool of monoclonal antibodies to A/WSN/33 HA. Viruses released into the culture medium were biologically cloned by plaque assay. The rescue of A/Udorn/HA into the A/WSN genetic background was monitored by immunoprecipitation of Udorn HA from virus-infected cells, and then the presence of the A/Udorn/72 HA RNA segment in the A/WSN/33 genetic background was confirmed by nucleotide sequence analysis of RNA segment 4 encoding HA. Both wild-type HA (A/Udorn/72 HA rescued into the A/WSN/33 background) and tail$^-$ HA (A/Udorn/72 tail$^-$ HA rescued into the A/WSN/33 background) transfectant viruses were obtained. The translational stop codon introduced into tail$^-$ HA was shown to be present in the HA RNA segment of the tail$^-$ HA transfectant (see below in Figure 8C).

Wild-type HA and tail$^-$ HA transfectant viruses were plaque purified three times on MDCK cells, the viruses propagated in eggs, and viruses purified on sucrose density gradients. The polypeptide composition of the wild-type HA and tail$^-$ HA transfectant viruses was compared to that of purified A/WSN/33 and A/Udorn/72 virions. Polypeptides were separated by electrophoresis on polyacrylamide gels and visualized by staining with Coomassie brilliant blue. The tail$^-$ HA species was found to migrate significantly faster than the wild-type HA (Figure 2A). More importantly, the relative abundance of the identifiable virion polypeptides (HA, NP and M) in the tail$^-$ HA rescued virus was approximately equivalent to that found in the control wild-type HA rescued virus. The immunological specificity of the rescued A/Udorn tail$^-$ HA was confirmed by probing immunoblots with an antiserum specific to A/Udorn/72 HA and finding reactivity with the A/Udorn HA species, but not the A/WSN HA species (Figure 2B).

To examine further the synthesis of tail$^-$ HA virus-specific polypeptides, HA species from virus-infected cells

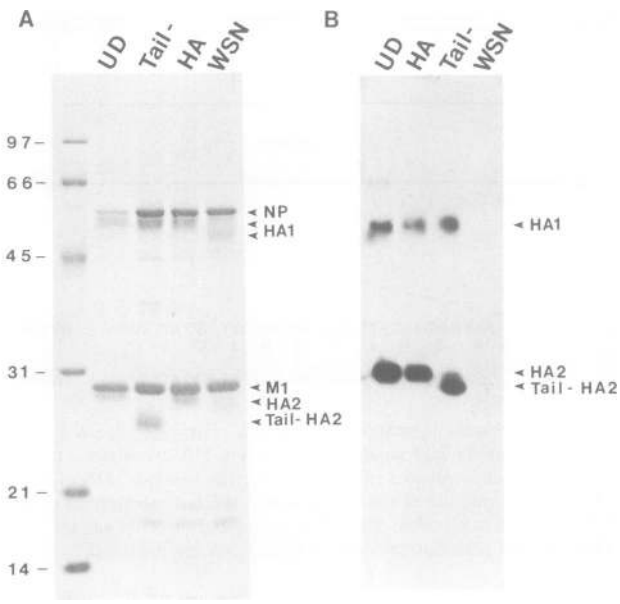

Fig. 2. The tail$^-$ HA is efficiently incorporated into virions. Viruses as indicated were grown in embryonated eggs, purified through sucrose gradients and viral polypeptides separated on 15% SDS–polyacrylamide gels. (**A**) Polypeptides were stained with Coomasie brilliant blue and gels photographed. (**B**) Polypeptides were transferred electrophoretically to an immunoblot membrane and the blot incubated with a polyclonal antiserum specific for A/Udorn/72 HA (SP31). The tail$^-$ HA_2 has a faster mobility compared to wild-type HA_2, as indicated. UD, A/Udorn/72 virus; WSN, A/WSN/33 virus; HA, wild-type HA transfectant virus; Tail$^-$, Tail$^-$ HA transfectant virus. Note the lack of reactivity of antiserum with HA species in lane WSN.

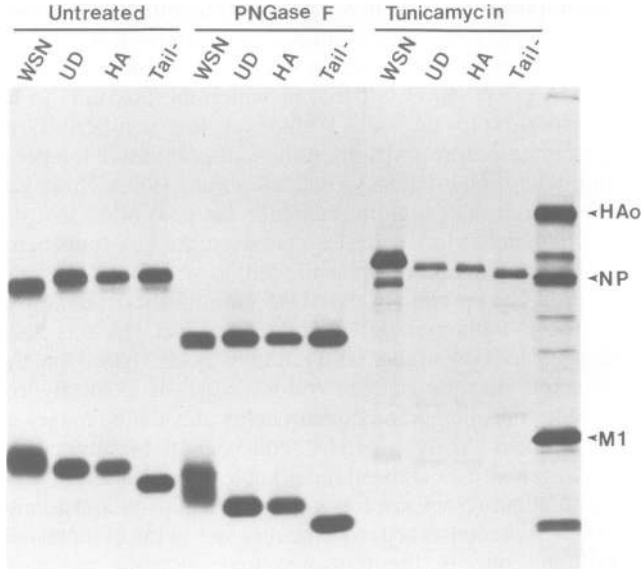

Fig. 3. The altered mobility of tail$^-$ HA2 is not due to a change in glycosylation. Left and middle: CV-1 cells were infected with the viruses as indicated and at 5 h p.i. were labeled with Trans[^{35}S] label for 60 min. Cells were harvested, and HA_0 was cleaved to HA_1 and HA_2 by addition of TPCK–trypsin. HA was immunoprecipitated with antiserum specific for A/WSN/33 HA or antiserum specific for A/Udorn/72 HA. One aliquot of the immune complex was digested with PNGase F and the other aliquot mock treated (untreated). Polypeptides were analyzed on 15% SDS–polyacrylamide gels. Note that the deglycosylation of A/WSN/33 HA_2 was not complete in this experiment. Right: CV-1 cells were infected with the viruses indicated and at 4 h p.i. cells were treated with tunicamycin (2 μg/ml) for 2 h and then labeled with Trans[^{35}S] label in the presence of tunicamycin. The cell lysates (omitting treatment with TPCK–trypsin) were immunoprecipitated by using an HA-specific antiserum. UD, A/Udorn/72 virus; WSN, A/WSN/33 virus; HA, wild-type HA transfectant virus; Tail$^-$, Tail$^-$ HA transfectant virus.

were cleaved with trypsin and immunoprecipitated with antibody specific for either the A/Udorn/72 HA or A/WSN/33 HA. The tail$^-$ HA_2 species again showed a distinct mobility difference from HA_2 of wild-type HA transfectant virus, or HA_2 of A/Udorn/72 or A/WSN/33 viruses (Figure 3, lanes untreated). To rule out the possibility that the difference in migration of the tail$^-$ HA_2 species in comparison to other HAs analyzed was due to the trivial explanation of altered addition of carbohydrate chains, radiolabeled HA species were deglycosylated by digestion with peptide *N*-glycosidase F. As shown in Figure 3 (lanes PNGase F), deglycosylated tail$^-$ HA_2 migrated faster than deglycosylated HA_2 of the other viruses. In this experiment, digestion of A/WSN/33 HA_2 with peptide *N*-glycosidase F did not go to completion. To examine further the mobility difference of the tail$^-$ HA in comparison with wild-type HA, virus-infected cells were metabolically labeled in the presence of tunicamycin, an inhibitor of addition of N-linked carbohydrate. HA_0 of tail$^-$ HA virus had a faster mobility than HA_0 of A/Udorn/72 virus (Figure 3, lanes tunicamycin). Thus, the faster mobility of tail$^-$ HA_2 shown in Figures 2 and 3 is consistent with the absence of 10 residues from the cytoplasmic tail of tail$^-$ HA_2.

Immunogold electron microscopy of tail$^-$ HA virus indicates a normal HA distribution

If the cytoplasmic tail of HA plays a major role in the viral assembly or the budding process, the tail$^-$ HA transfectant might exhibit a different morphology or possess altered HA content in comparison with wild-type virus. To examine the morphology of transfectant virions and the relative abundance of HA spikes in wild-type and tail$^-$ HA transfectants, viruses purified from sucrose gradients were absorbed onto grids and stained with an HA-specific monoclonal antibody. Following reaction with a secondary antibody coupled to 10 nm gold particles, the virus was negatively stained with phosphotungstic acid. It was found that the wild-type and tail$^-$ HA transfectant viruses exhibited similar morphology with respect to the size, shape and number of glycoprotein spikes (Figure 4). The level of labeling of both wild-type and tail$^-$ HA transfectant viruses with HA-specific monoclonal antibodies indicates that the relative abundance of HA spikes in the viral envelope of both viruses is comparable. When similar preparations were stained with a monoclonal antibody specific for the HN glycoprotein of paramyxovirus SV5, almost no background staining was observed (results not shown). These data suggest that the absence of the cytoplasmic tail of HA affects neither the incorporation of HA molecules into the viral envelope nor the morphology or the HA content of progeny virus.

Tail$^-$ HA rescued virus does not contain an A/WSN/33 HA membrane anchor and cytoplasmic tail

The tail$^-$ HA transfectant virus was plaque purified three times and both a linear relationship of plaques to virus

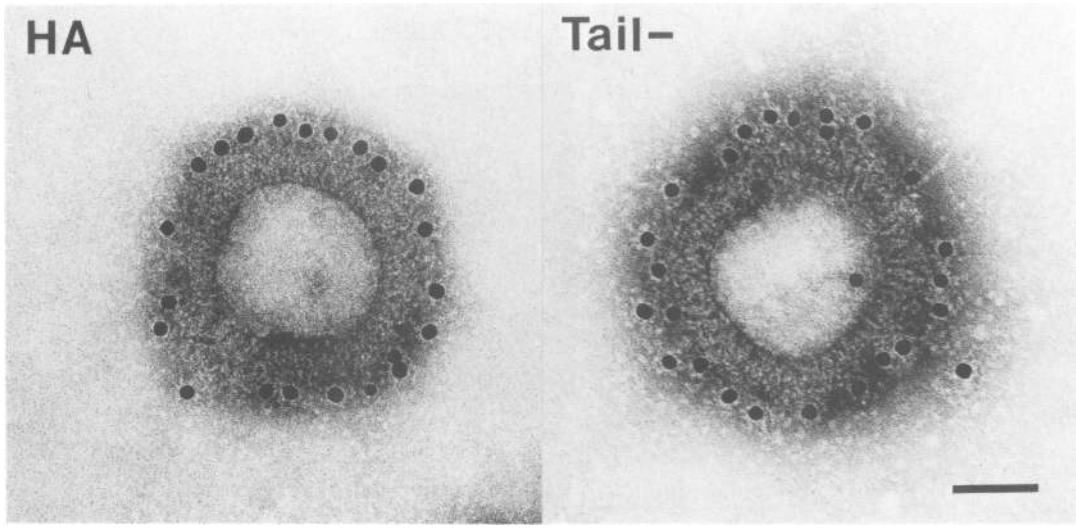

Fig. 4. Immunoelectron microscopy of the wild-type HA and tail$^-$ HA transfectant viruses. Wild-type and tail$^-$ HA transfectant viruses were grown in embryonated eggs, purified on sucrose gradients and absorbed onto Ni grids and incubated with an HA-specific monoclonal antibody (D6/1). Grids were washed in TBS and stained with goat anti-mouse IgG coupled to 10 nm colloidal gold. Prior to examination, virus preparations were negatively stained with phosphotungstic acid. Both wild-type HA and tail$^-$ HA transfectant viruses showed a comparable level of labeling with anti-HA antibody. Furthermore, there were no gross morphological changes evident between the wild-type HA and tail$^-$ HA transfectant viruses. Bar, 50 nm.

dilution and equal plaquing efficiency at each passage were obtained. Thus, tail$^-$ HA virus would be expected to be genetically homogeneous. Nonetheless, we considered it necessary to exclude the possibility of the presence of the A/WSN/33 HA cytoplasmic tail (and transmembrane domain) in the tail$^-$ HA rescued virus, which might act *in trans* for the assembly of the tail$^-$ HA virus.

The composition of the genome RNA segments of both wild-type HA and tail$^-$ HA transfectant viruses was analyzed by separation on a polyacrylamide gel. As shown in Figure 5A, both tail$^-$ HA and wild-type HA viruses contained the expected eight genome RNA segments of influenza virus. An additional RNA band migrating faster than RNA segment 8 was observed in wild-type HA transfectant virions, but not in tail$^-$ HA transfectant, and the band probably represents a defective-interfering RNA species. More importantly, additional small RNA bands were not observed in tail$^-$ HA transfectant virus, although the presence of a very small RNA species, such as a truncated A/WSN/33 HA RNA, may not be detected using this gel system. To examine further for the presence of an A/WSN/33 HA-specific RNA fragment in the rescued virus, viral RNA was reverse transcribed and amplified by a PCR method using either primers common to A/WSN/33 and A/Udorn/72 which yielded a 314 (WSN) or 327 (Udorn) bp DNA fragment, or primers specific for A/WSN/33 HA which yielded a 168 bp fragment. No 168 nucleotide species was produced from A/Udorn/72 viral RNA or from RNA of the two rescued viruses (Figure 5B), even after a prolonged number of PCR cycles (data not shown). Thus, neither wild-type HA transfectant nor tail$^-$ HA transfectant contains an A/WSN/33 HA RNA fragment which could encode the A/WSN/33 HA_2 transmembrane domain and cytoplasmic tail.

Another means of examining for the presence of the A/WSN/33 membrane anchor and cytoplasmic tail domains in tail$^-$ HA virus is to perform immunoprecipitations using a polyclonal serum specific for the A/WSN/33 cytoplasmic tail (kindly provided by Angela Wandinger-Ness and Kai Simons). Influenza virus A/WSN/33 HA_1 contains nine cysteine residues, HA_2 six cysteine residues, and the HA transmembrane and cytoplasmic tail three cysteine residues. Thus, by labeling with [^{35}S]cysteine and quantifying autoradiogram exposures, it is possible to set an upper limit for the presence of an HA-related polypeptide. On 17.5% SDS–polyacrylamide gels, the dye front migrates as an apparent mol. wt of 3 kDa and the predicted size of the A/WSN/33 transmembrane domain and cytoplasmic tail is ~4–5 kDa and with an assumed apparent size >5 kDa due to the effect of the three covalently linked palmitate groups to this domain. In addition, by using this gel system, an ~40 residue fragment of the influenza virus M_2 protein, including the transmembrane domain, has been identified (Zebedee *et al.*, 1985). The A/WSN/33 anti-tail serum precipitated HA_2 of A/WSN/33 (and HA_1 because of the disulfide bond linking HA_1 and HA_2). However, when the WSN tail antibody was used to precipitate lysates of tail$^-$ HA or wild-type HA-infected cells, no HA_2-related species of any size were detected, given the caveat that the anti-tail serum can recognize the putative fragment. Assuming antibody recognition, the upper limit of detection is calculated to be 1/500 of the level of HA_2. Thus, taken together, these control experiments indicate that the tail$^-$ HA virus does not express the A/WSN/33 HA cytoplasmic tail.

The interpretation of the data concerning the assembly of tail$^-$ HA virus would be compromised if suppression of termination at the artificially introduced TGA codon in tail$^-$ HA occurred at a significant level. If this were the case, it would be expected that translation would continue to the termination codon that is normally used for HA_2 and molecules of the normal size for HA_2 would be

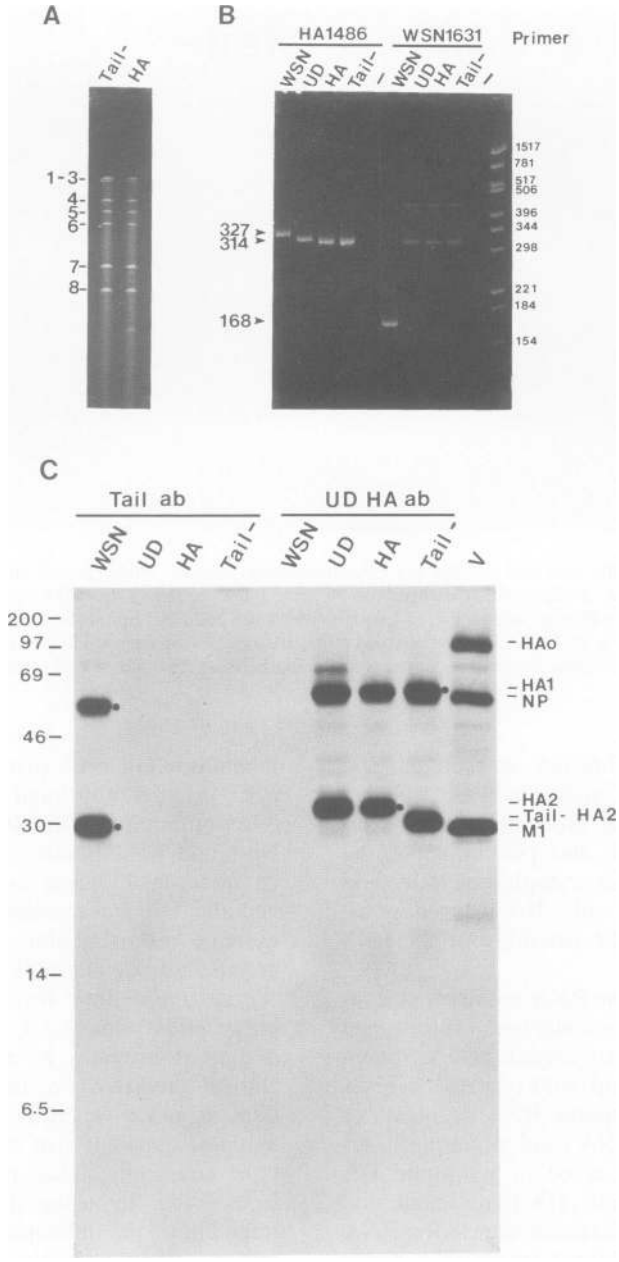

Fig. 5. The tail$^-$ HA transfectant virus contains neither A/WSN/33 derived HA RNA nor A/WSN/33 derived HA_2 protein. (**A**) Viral RNA segments of tail$^-$ HA and wild-type HA transfectant viruses were phenol extracted from purified virions, separated on a 3.5% polyacrylamide gel containing 8 M urea and visualized by staining with ethidium bromide. The eight RNA segments of both the tail$^-$ HA transfectant and wild-type HA transfectant viruses are indicated; no additional bands were detected in tail$^-$ HA transfectants. (**B**) PCR analysis of viral HA RNAs. The virion RNA segments were transcribed with reverse transcriptase and using as primer a mRNA sense oligonucleotide HA1486 (HA nucleotides 1486–1502) which is conserved in sequence between A/WSN/33 and A/Udorn/72. cDNAs were amplified by using either a mRNA sense oligonucleotide primer HA1486 or by using a mRNA sense primer specific for HA of strain A/WSN/33 [WSN 1631 (nucleotides 1631–1655) specific for the HA transmembrane domain] and a vRNA sense oligonucleotide (HAendT7) specific for the immediate 5′ end of the vRNA segment. PCR DNA products were analyzed on a 6% polyacrylamide gel. No DNA of 168 nucleotides in length, derived from A/WSN/33 RNA, was observed in tail$^-$ HA and wild-type HA transfectants. Some 314 nucleotide DNA was amplified from the reaction in HA1631 primer due to some residual HA1486 from the reverse transcriptase reaction. (**C**) Immunoprecipitation of radiolabled proteins by polyclonal antibody specific to the A/WSN/33 HA cytoplasmic tail. CV-1 cells were infected with viruses as indicated and labeled at 5 h p.i with [^{35}S]cysteine for 1 h. Cells were lysed and HA_0 cleaved with TPCK–trypsin and HA species immunoprecipitated with affinity-purified polyclonal antiserum specific for the A/WSN/33 HA cytoplasmic tail (Tail ab) or with polyclonal antiserum to A/Udorn/72 HA (UD HA ab). Polypeptides were separated on 17.5% SDS–polyacrylamide gels containing 4 M urea. No A/WSN/33 HA_2 or a species of 4–5 kDa, which would be the predicted size of the A/WSN/33 HA_2 combined transmembrane and cytoplasmic tail domains, was detected in tail$^-$ HA and wild-type HA transfectants even on prolonged exposures of the autoradiographs. Note that in this gel system A/WSN/33 HA_1 and HA_2 migrated faster than A/Udorn/72 HA_1 and HA_2, and this is indicated by dots adjacent to the polypeptide species.

detected in tail$^-$ HA virus-infected cells. To set an upper limit of detection of suppression of termination of HA tail$^-$, HA species were immunoprecipitated from tail$^-$ HA virus-infected cell, serial dilutions made and polypeptides analyzed by SDS–PAGE. In tail$^-$ HA transfectant-infected CV-1 cells, tail$^-$ HA_2 molecules could be detected

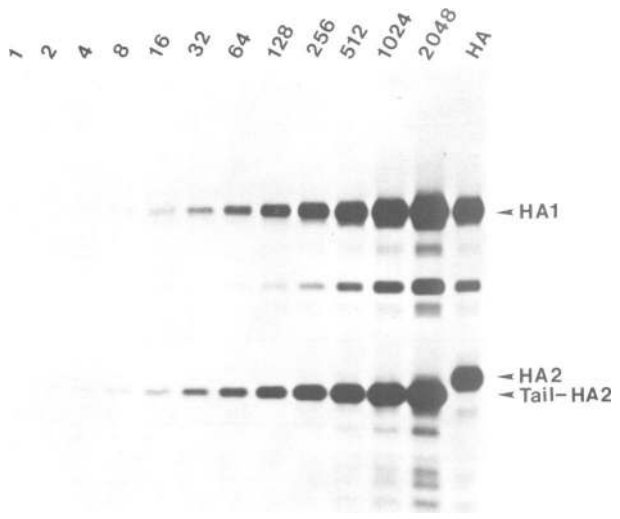

Fig. 6. Suppression of translational termination of tail$^-$ HA is not detectable. CV-1 cells were infected with tail$^-$ HA virus or wild-type HA virus and at 5 h p.i. were labeled with Trans[^{35}S] label for 60 min. Cells were harvested and HA_0 was cleaved to HA_1 and HA_2 by addition of TPCK–trypsin. HA was immunoprecipitated with antiserum specific for A/Udorn/72 HA. Immune complexes were released from protein A-Sepharose beads with SDS, and for tail$^-$ HA serial 2-fold dilutions of the immunoprecipitated proteins were made. Polypeptides were analyzed on 15% SDS–polyacrylamide gels. Numbers indicate the inverse of the dilution from 1 (the lowest) to 2048 (the highest).

at 1:2048 dilution, while no polypeptide corresponding to intact HA was detected on the gel (Figure 6). Since an influenza virus particle generally contains ~300–500 trimeric HA molecules (Lamb and Choppin, 1976), it seems unlikely that the tail$^-$ HA rescued virus contains non-truncated HA molecules at a meaningful level in the virion.

Infectivity and neutralization of tail$^-$ HA transfectant virus

The infectivity of tail$^-$ HA and wild-type HA transfectant viruses grown in MDCK cells and embryonated eggs was determined by plaque assay in MDCK cells. The infectivity was standardized to HA titer (note: HA distribution in tail$^-$ HA virus appeared normal in Figures 2 and 4). The p.f.u. to HA unit ratio of tail$^-$ HA transfectants produced from MDCK cells was ~2-fold lower than wild-type HA virus grown in MDCK cells, and for tail$^-$ HA virus grown in eggs it was approximately equivalent to that of wild-type HA transfectants grown in embryonated eggs (Table I). In addition, the infectious virus particle yield obtained from a single plaque of tail$^-$ HA transfectant virus on subsequent plaquing was 2- to 5-fold lower than for wild-type HA transfectant virus (400 versus 2000 plaques per plaque in 1 ml, respectively). Interestingly, the plaque size of tail$^-$ HA transfectant virus on MDCK cells was similar to that of wild-type HA transfectant virus. However, the tail$^-$ HA plaques had fuzzy edges in comparison to the discrete plaques of wild-type HA transfectant virus. To examine for the ability of tail$^-$ HA virus to be neutralized by antibody, wt and tail$^-$ HA viruses were pre-incubated with 0.25% SP31 HA antiserum at 4°C for 60 min and were then used to infect MDCK cells. After 60 min adsorption, cell monolayers were overlaid with 1% agarose/MEM/1 μg/ml *N*-acetyl trypsin. Complete neutralization of plaque formation was observed in cells infected with either the tail$^-$ HA transfectant or the wild-type HA transfectant that had been pre-incubated with the antiserum. Thus, these data indicate that both viruses were efficiently neutralized at the concentration of antibody used.

Kinetics of intracellular transport and cell surface expression of tail$^-$ HA

It was previously shown that the deletion of the cytoplasmic domain of HA molecules affects its rate of intracellular transport and cell surface expression when the HA cDNA was expressed by using a recombinant SV40 virus or a vaccinia–T7 polymerase expression system (Doyle *et al.*, 1985, 1986; Simpson and Lamb, 1992). To determine whether a similar effect is observed for the tail$^-$ HA virus when expressed in influenza virus-infected cells, an analysis of the kinetics of resistance of HA carbohydrate chains to digestion with endo H, indicative of transport to the medial Golgi apparatus, was performed. As shown in Figure 7A, for both wild-type HA and tail$^-$ HA there was a loss of radioactivity during the chase period due to HA being released into budding virions (data not shown). Nonetheless, although making a kinetic analysis more complicated, the data indicate that the kinetics of transport of tail$^-$ HA to the medial Golgi apparatus is delayed ($t_{1/2}$ ~50 min) in comparison with wild-type HA ($t_{1/2}$ ~20 min). Thus, these data are very similar to those obtained previously when tail$^-$ HA was expressed by using the vaccinia virus–T7 polymerase system (Simpson and Lamb, 1992).

The rates of transport of wild-type HA and tail$^-$ HA to the cell surface were also compared. Virus-infected cells were radiolabeled with Trans[^{35}S] label for 10 min and chased for various periods and the cell monolayers incubated with TPCK–trypsin to cleave HA_0 molecules transported to the cell surface to HA_1 and HA_2. The amount of immunoprecipitable cleaved HA at each time point was quantified by using scanning densitometry, and the rate of transport of tail$^-$ HA was found to be slower ($t_{1/2}$ ~65 min) than that of wild-type HA ($t_{1/2}$ ~45 min) (Figure 7B), given the caveats discussed above concerning the loss of HA in the chase period due to the release of budding virions. The difference in the rate of transport of the tail$^-$ HA and wild-type HA to the cell surface is considerably less than the difference in rate of transport of the two molecules to the medial Golgi complex.

Quantification of budding of tail$^-$ HA transfected viruses from the plasma membrane

An immunoelectron microscopic examination of the budding of progeny virus from MDCK cells infected with either the wild-type or tail$^-$ HA transfectant viruses was performed to gain further insight into the ability of the viruses to assemble and bud. Infected MDCK cells at 5 h p.i. were incubated with A/Udorn/72 HA specific monoclonal antibody, and the primary antibody binding was visualized by staining with a goat anti-mouse secondary antibody coupled to 10 nm colloidal gold. Cells were fixed with 2% glutaraldehyde, post-fixed in 1% OsO4 and embedded in epoxy resin. MDCK cells infected with wild-

Table I. The infectivity of the rescued transfectant viruses

Virus	Expt	Host	p.f.u./ml ($\times 10^6$)	HAU/ml	p.f.u./HAU ($\times 10^4$)
WT HA	1	egg	87.5	2048	4.27
	2	egg	20.0	512	3.91
	3	egg	35.0	2048	1.71
	4	MDCK	4.6	512	0.92
Tail$^-$ HA	1	egg	18.5	512	3.61
	2	egg	20.0	512	3.91
	3	egg	20.0	512	3.91
	4	MDCK	1.2	256	0.47

type HA virus were found to exhibit consistently 2- to 3-fold more budding virus than cells infected with the tail$^-$ HA transfectant (Figure 8 and Table II). Budding was quantified by counting budding virus from ~600 mm of cell membrane, representing the results of three separate infections for both the wild-type and tail$^-$ HA transfectant viruses as described in Materials and methods.

Genetic stability of tail$^-$ HA transfectant virus

To investigate the genetic stability of the tail$^-$ HA virus, serial plaque-to-plaque passages on MDCK cells were performed. Single plaques were isolated, diluted and used to re-infect fresh MDCK cells successively for six passages. Viruses obtained from single plaques were then propagated in embryonated eggs. The maintenance of the deletion of the HA cytoplasmic tail was monitored by labeling the infected CV-1 cells with Trans[^{35}S] label, immunoprecipitation with HA specific antibody and separation of the proteolytically cleaved HA_1 and HA_2 on SDS–polyacrylamide gels. As shown in Figure 9A, for all six serial plaque passages of the virus, the absence of the HA cytoplasmic tail was maintained. However, in one unrelated egg-grown stock of tail$^-$ HA virus, two species of HA_2 were observed, one being the expected tail$^-$ HA2 species and the other having a mobility similar to that of the wild-type HA_2 (Figure 9B, lane R). To determine if this virus stock contained a reversion mutant, the nucleotide sequence of the viral HA RNA was examined. The viral RNA was extracted, reverse transcribed by using an HA specific primer and the resulting cDNA amplified by PCR. Sequence analysis of the cloned HA cDNAs showed that some of the cloned HA cDNAs contained a TGA to TGG mutation (encoding tryptophan) at the position of the stop codon introduced into tail$^-$ HA (Figure 9C). When this mixed virus stock was passaged either in embryonated eggs or in MDCK cells, the revertant virus outgrew the tail$^-$ HA virus (data not shown). Thus, these data suggest that although tail$^-$ HA transfectant virus can be successfully assembled and passaged, a cytoplasmic tail to HA is preferred.

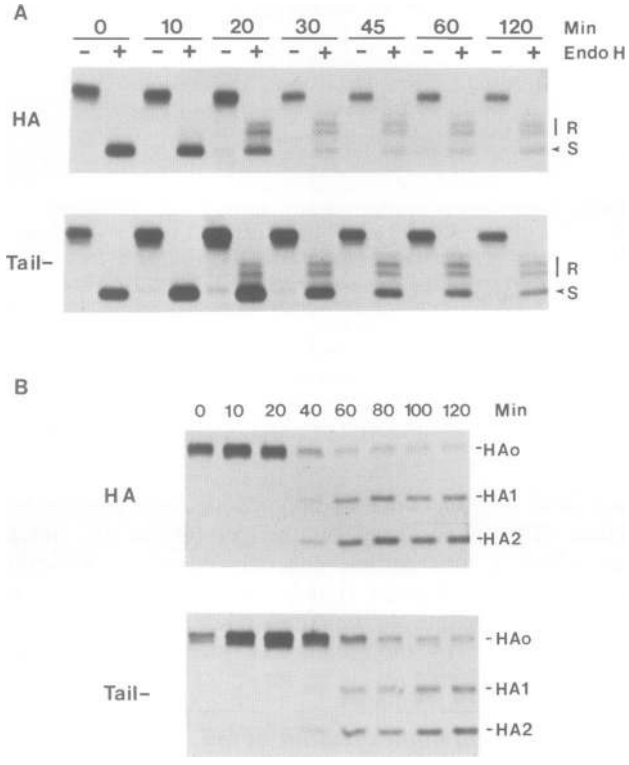

Fig. 7. Kinetics of transport of tail$^-$ HA and wt HA to the medial Golgi complex and the cell surface. (**A**) CV-1 cells were infected with wild-type HA and tail$^-$ HA transfectants and labeled with Trans[^{35}S] label at 5 h p.i. for 10 min, and then incubated in chase medium for varying periods as indicated. HA was immunoprecipitated with A/Udorn/72 HA-specific antiserum SP31 and digested with (+) or without (−) endo H for 18 h, and polypeptides analyzed on 10% SDS–polyacrylamide gels. R; endo H-resistant species. S; endo H-sensitive species. (**B**) Virus-infected CV-1 cells were labeled as in (A) above and incubated in chase medium for the times indicated. The cell monolayers were then incubated with 50 μg/ml TPCK–trypsin at 4°C for 60 min, washed with 10% serum in PBS. HA was precipitated with polyclonal antiserum SP31 and polypeptides analyzed on 10% SDS–polyacrylamide gels. Only the relevant portions of the autoradiographs are shown.

Discussion

The study reported here demonstrates that influenza virus which lacks the cytoplasmic domain of HA can be assembled and replicated quite efficiently. Previously, in a study on HA transport-defective temperature-sensitive mutant influenza virus, A/WSN/33 ts61s, it was found that spikeless virions lacking HA could be produced efficiently at the non-permissive temperature (Pattnaik *et al.*, 1986). However, it was not known whether these spikeless virions contained the cytoplasmic tail and transmembrane domain of HA, which could act as nucleating points for assembly. In another study where tail$^-$ HA molecules were used to complement the A/WSN/33 ts61s virus at the non-permissive temperature, by using the transient vaccinia virus–T7 polymerase expression system, it was found that very little released virus was infectious (Simpson and Lamb, 1992). The lowered surface

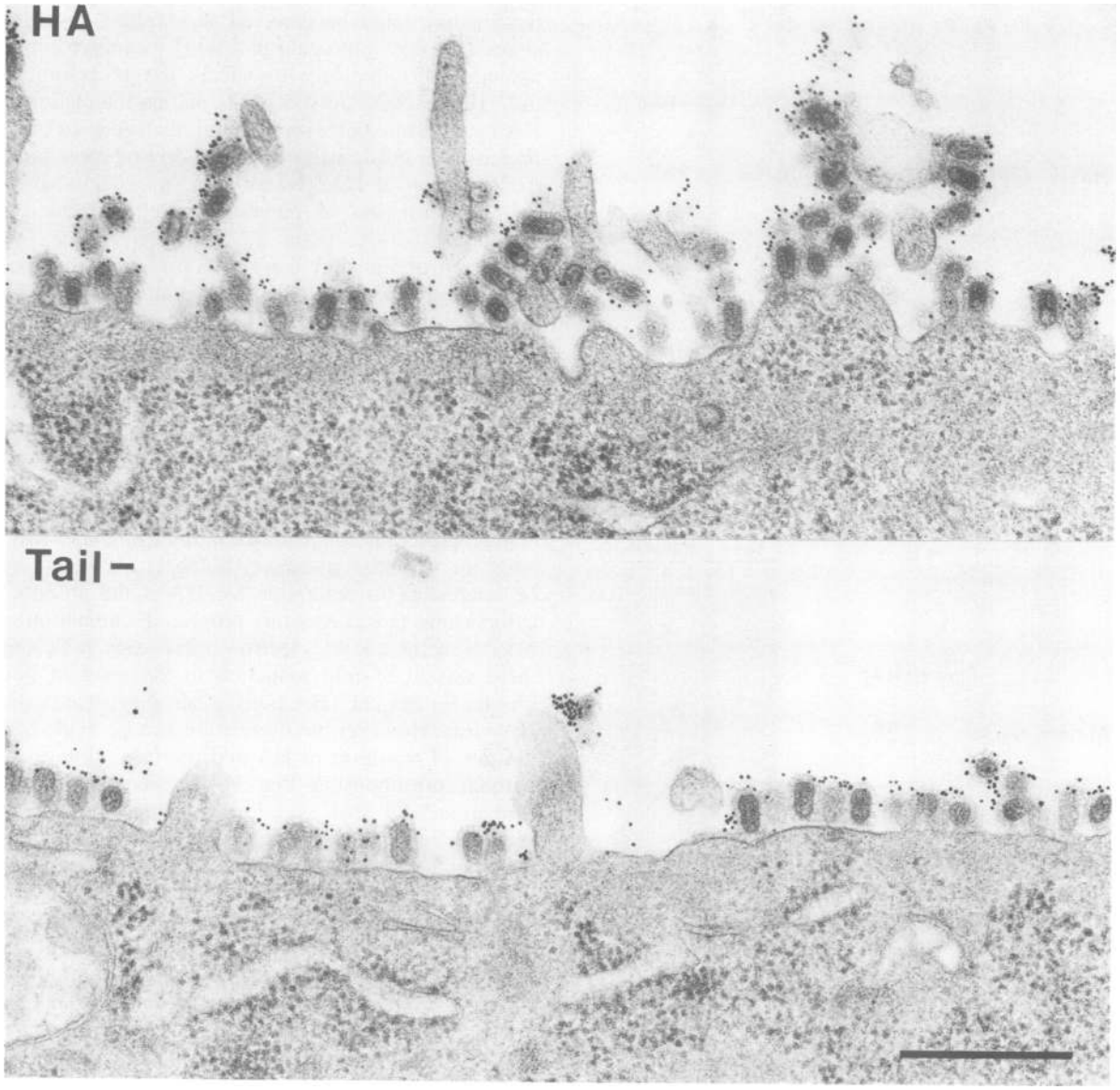

Fig. 8. Efficiency of budding of tail$^-$ HA transfectant progeny virus from the plasma membrane. Wild-type or tail$^-$ HA transfectant virus-infected MDCK cells at 5 h p.i. were incubated at 4°C and reacted with an HA-specific monoclonal antibody followed by goat anti-mouse IgG secondary antibody coupled to 10 nm colloidal gold. Cells were fixed with glutaraldehyde, post-fixed with osmium tetroxide and embedded in epoxy resin. Thin sections were stained with uranyl acetate and lead citrate. Typically, MDCK cells infected with the wild-type virus HA transfectant (HA) showed 2- to 3-fold more progeny on the cell surface than the tail$^-$ HA transfectant virus (tail$^-$). Bar, 0.5 μm.

Table II. Quantification of budding virions in MDCK cells for wild-type HA and tail$^-$ HA transfectant viruses

Virus	Wild-type HA			Tail$^-$ HA		
	Expt 1	Expt 2	Expt 3	Expt 1	Expt 2	Expt 3
Total length (μm)	238	227	298	125	191	222
Virus number	915	1525	2254	236	434	709
Virus number/100 μm	384.5	671.8	756.4	188.8	228.2	319
	(Average 604.2 ± 159)			(Average 245 ± 54)		

expression of tail$^-$ HA molecules because of the slower transport kinetics and the very narrow time period in which it was possible to perform those experiments, (the time period necessitated by the difficulty of working with a vaccinia virus and influenza virus co-infection), may explain the difference in results beween the earlier study and that reported here. The generation of a tail$^-$ HA transfectant virus by using reverse genetics would be expected to be genetically homogeneous. In addition, experiments designed to eliminate possible artifacts indicate tail$^-$ HA virus neither encoded nor contained a cytoplasmic tail and transmembrane domain from the

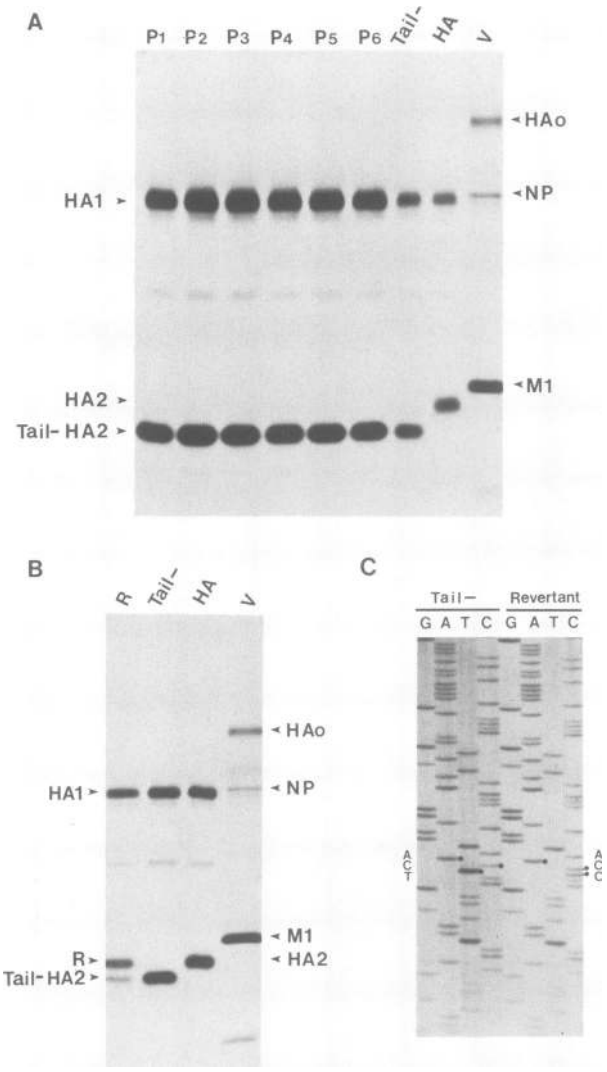

Fig. 9. Analysis of the genetic stability of tail$^-$ HA transfectant virus. (**A**) Tail$^-$ HA transfectant virus was serially plaque passaged for six generations (P1–P6) in MDCK monolayers, and virus from a single plaque at each plaque passage was propagated in embryonated eggs. CV-1 cells were infected with the amplified, plaque-purified virus and infected cells were labeled with Trans[^{35}S] label. HA_0 was cleaved with TPCK–trypsin and immunoprecipitated with polyclonal antiserum SP31. All six passages of tail$^-$ HA transfectants were found to maintain the tail$^-$ truncation. (**B**) Characterization of a tail$^-$ HA revertant virus. Viruses as indicated were grown in embryonated eggs and were used to infect CV-1 cells. Trans[^{35}S] labeled cell lysates were immunoprecipitated with A/Udorn/72 HA specific antiserum SP31 and analyzed on 15% SDS–polyacrylamide gels. In lane R, both the normal tail$^-$ HA_2 polypeptide species and a species (R) similar in size to the wild-type HA_2 were observed. R, mixed virus stock containing tail$^-$ HA and a revertant virus; tail$^-$, tail$^-$ HA transfectant virus; HA, wild-type HA transfectant virus. (**C**) Viral RNA was extracted from the virions containing two HA_2 species, its cDNA amplified by PCR, molecularly cloned and the nucleotide sequence of the region encoding the HA cytoplamsic tail determined. Sequencing of the cloned DNA of the revertant from the 5′ end of the viral sense strand showed that at the position where a translation stop codon had been introduced to make tail$^-$ HA, a point mutation within TGA had occurred (labeled as TCA in the viral sense) making the codon TGG (CCA in the viral sense) encoding tryptophan.

parental A/WSN/33 virus. Another possible artifact would be the read-through of the introduced translational termination codon used to generate tail$^-$ HA. However, reconstruction experiments indicate that no suppression of termination could be detected at a 1:2048 level, which suggests it does not occur at a level meaningful to affect assembly of influenza virus. Thus, the generation of the tail$^-$ HA rescued virus suggests that an interaction of the HA cytoplasmic tail with the viral nucleocapsid or matrix protein does not constitute a major driving force for either incorporation of HA glycoprotein spikes into virions or for the formation of budding particles at the plasma membrane.

The rate of transport of tail$^-$ HA glycoprotein molecules both in tail$^-$ HA transfectant virus-infected cells, and as discussed above when tail$^-$ HA was expressed from cDNA using the vaccinia virus–T7 polymerase expression system (Simpson and Lamb, 1992), was found to be delayed in comparison to wild-type HA. The lack of a tail does not affect trimerization (Simpson and Lamb, 1992), and thus it suggests that the HA cytoplasmic domain facilitates rapid and efficient transport between the ER and medial Golgi complex. Recently, it has been shown that the VSV G glycoprotein is concentrated in the ER at sites that form buds for vesicular transport (Balch *et al.*, 1994). It will be interesting to determine for HA if the absence of a cytoplasmic tail affects this process. Examination of the plasma membrane by electron microscopy indicated that there was a 2.5-fold reduction in the level of budding virions for the tail$^-$ HA transfectant virus than wild-type HA virus. However, no correlation can be made between the rate of transport of HA and the formation of virions without presupposing that HA is required for virion formation. All that is known at present is that HA molecules containing foreign cytoplasmic tails and foreign transmembrane domains fail to be incorporated into virus particles that contain a normal HA species (Naim and Roth, 1993).

The morphology of the tail$^-$ HA rescued virus appeared normal with respect to shape and distribution of HA spikes, and the polypeptide composition of virions showed an unchanged incorporation of tail$^-$ HA molecules. Thus, it seemed reasonable to use the standard assay of hemagglutination units as a measure of physical particles. The infectivity (p.f.u.) to HA units ratio for tail$^-$ HA virus and wild-type HA virus grown in embryonated eggs was very similar. For viruses grown in MDCK cells, tail$^-$ HA virus had an ~2-fold lower p.f.u. to HA units ratio than wild-type HA virus. Nonetheless, the finding of a tail$^-$ HA revertant virus (the premature termination codon reverted to a codon for tryptophan) which out-grew the tail$^-$ HA virus indicates that a HA cytoplasmic tail, although not necessary for virus replication, does confer a growth advantage. This finding correlates with those of another study, as when the ability of different HAs to compete for space in the influenza virus A/WSN/33 envelope was tested, it was found that A/Japan/57 tail$^-$ HA was incorporated into particles with only ~50% of the efficiency of A/Japan/57 wild-type HA (Naim and Roth, 1993).

It remains to be determined if the tail$^-$ HA rescued virus has all the biochemical properties of wild-type HA virus. From the data presented here, it is clear that the covalent linkage of palmitate to the two conserved HA cytoplasmic tail cysteine residues is not essential for virus infectivity. However, in one study the finding that

modification of these HA cysteine residues severely inhibited fusion activity (Naeve and Williams, 1990) suggests the possibility that the tail$^-$ HA virus could have an altered rate of fusion, and this possibility remains to be determined. Recently, it has been shown that the HA transmembrane domain is required to cause complete membrane fusion as HA anchored by a glycolipid anchor only causes incomplete hemi-fusion of bilayers (Kemble *et al.*, 1994) and it is possible that an alteration to the cytoplasmic tail may perturb the molecular structure of the transmembrane domain.

The data described here indicate that to understand the assembly of influenza virus, in addition to studying the role of the HA transmembrane domain, the roles of the two other influenza virus integral membrane proteins (NA and M_2 protein) must be investigated. Despite the possibility that HA-spikeless A/WSN/33 ts61s virions released from cells at the non-permissive temperature may contain an HA transmembrane domain and cytoplasmic tail fragment, the particles contained twice the normal amount of NA (Pattnaik *et al.*, 1986). Other intriguing observations that may relate to a functional role of the NA cytoplasmic tail in virus budding are: (i) the NA$^-$ influenza virus produced by Liu and Air (1993) retained an RNA fragment which has the potential to encode the cytoplasmic tail of NA and (ii) the report of negative data that it was not possible to obtain a tail$^-$ NA transfectant virus (Bilsel *et al.*, 1993). The influenza virus M_2 protein is a minor component of the viral envelope (Zebedee and Lamb, 1988) and its cytoplasmic tail is relatively long, containing 54 residues (Lamb *et al.*, 1985). An interaction of the M_2 protein with the M_1 protein has been suggested, based on the observations that mutations in the M_2 cytoplasmic tail or the M_1 protein prevent the growth restriction caused by a monoclonal antibody to the M_2 extracellular domain (Zebedee and Lamb, 1989). An interaction of M_2 protein with M_1 protein or nucleocapsid proteins is also supported by the observation that M_2 protein co-sedimented with M_1 protein-containing nucleocapsids (Bron *et al.*, 1993). A coupling of reverse genetics procedures for influenza virus with biochemical approaches should yield essential information on the viral assembly process.

Materials and methods

Cells and viruses

Madine–Darby bovine kidney (MDBK) cells, Madine–Darby canine kidney (MDCK) cells and CV-1 cells were maintained in Dulbecco's modified Eagle's medium (DME) supplemented with 10% fetal bovine serum. Influenza virus A/WSN/33 was propagated in MDBK cells, influenza viruses A/PR8/34 and A/Udorn/72 were grown in 11 day embryonated chicken eggs. RNP transfections were performed in MDBK cells and plaque assay purification of viruses was performed in MDCK cells.

Construction of plasmids

To generate viral sense RNA transcripts of the influenza virus A/Udorn/72 HA for *in vitro* reconstitution of HA–RNP complexes, a full-length cDNA copy of A/Udorn/72 HA (Simpson and Lamb, 1992) was subcloned into the pUC19 vector. A bacteriophage T7 RNA polymerase promoter was inserted adjacent to the HA cDNA such that RNA transcripts could be synthesized in the viral RNA sense, and an *Ear*I site was inserted at the other end of the HA insert to obtain a unique and precise site for the linearization of the template (see Figure 1). The plasmid was designated pT7HA. Recombinant DNA technology was performed by standard PCR and cloning techniques (Ausubel *et al.*, 1994). The nucleotide sequence of DNA fragments subjected to PCR was confirmed by the dideoxynucleotide chain-terminating method (Sanger *et al.*, 1977). The tail$^-$ HA cDNA (pT7HAtail$^-$), which contains a translational stop codon in place of the lysine residue at the boundary of the HA transmembrane domain and cytoplasmic tail (Figure 1), was synthesized by PCR using as template pT7HA DNA.

Rescue of transfectant virus containing A/Udorn/72 HA RNA segment

Influenza virus nucleoprotein (NP) and the three polymerase (P) proteins were purified from virus A/PR8/34 as described previously (Parvin *et al.*, 1989). The reconstituted HA–RNP complex was made by *in vitro* transcription of *Ear*I-digested pT7HA or pT7HAtail$^-$ essentially as described by Enami and Palese (1991). The rescued transfectant viruses were selected using a mixture of monoclonal antibodies to A/WSN/33 HA (108/2, 157/2, 333/5, 410/2, 521/1 and 570/6; gifts of Kathleen Coelingh) essentially as described by the method of Li *et al.* (1992). Briefly, the HA–RNP was made by *in vitro* transcription of 1 μg of *Ear*I-digested pT7HA or pT7HAtail$^-$ in the presence of 10 μl of purified NP and the three P proteins in a final volume of 25 μl. Subconfluent MDBK cells in 35 mm culture dishes were infected with A/WSN/33 (m.o.i. of 1) for 1 h at room temperature and the monolayers were treated with 0.3 mg/ml DEAE-dextran and 0.5% dimethyl sulfoxide (DMSO) in phosphate-buffered saline (PBS)–gelatin (0.1 mg/ml gelatin in phosphate-buffered saline lacking Ca^{2+} and Mg^{2+}) for 30 min at room temperature. The solution was removed, and 125 μl of PBS–gelatin containing 25 μl of reconstituted HA RNP was added and the cells incubated for 1 h at room temperature. The solution was removed and the cells were overlaid with DME containing 0.5% bovine serum albumin and incubated at 37°C for 16–18 h. The culture supernatant was used to infect MDCK cells in the presence of 0.1% of a pooled monoclonal antibody mixture specific for A/WSN/33 HA and incubated for 2 or 3 days. The selection of the rescued virus on MDCK cells was repeated and plaques isolated in the presence of a pooled monoclonal antibodies mixture to A/WSN/33 HA. Resulting plaques were plaque purified three times on MDCK monolayers before being propagated in embryonated chicken eggs.

Viral RNA extraction, PCR and nucleotide sequencing

Virions grown in embryonated eggs were purified on 20–60% sucrose gradients (Paterson and Lamb, 1993). Viral RNA was extracted with phenol, phenol/chloroform and precipitated with ethanol. Viral RNA genomic segments were analyzed on 3.5% polyacrylamide gels containing 8 M urea and visualized by staining with 0.5 μg/ml ethidium bromide in 0.5 M NaOAc. To amplify the HA RNA segment by PCR, viral RNA was reverse transcribed by using avian myeloblastosis virus reverse transcriptase using HA specific primers (see text), and DNA was synthesized by 25 cycles of PCR (94°C for 40 s, 50°C for 40 s and 72°C for 40 s). The DNA fragment was either sequenced directly (Winship, 1989) or cloned into the pUC19 vector and sequenced by the dideoxynucleotide chain-terminating method (Sanger *et al.*, 1977).

Pulse labeling of infected cells, immunoprecipitation, polyacrylamide gel electrophoresis (SDS–PAGE) and immunoblotting

Monolayers of CV-1 cells were infected with viruses at a m.o.i. of 5–10, incubated in DME deficient in Cys and Met (DME Met$^-$/Cys$^-$) for 30 min and then labeled with Trans[^{35}S] label (100 μCi/ml) for 60 min unless otherwise stated. To cleave HA_0 to HA_1 and HA_2, cells were washed with PBS and lysed in 0.5 ml of 1% NP-40/0.1% SDS/50 mM Tris–HCl (pH 7.4). The lysate was clarified by centrifugation (55 000 r.p.m., 10 min, Beckman TLA100.2) and incubated with 5 μg/ml L-(tosylamido-2-phenyl) ethyl chloromethyl ketone (TPCK)–trypsin (Worthington Biochemicals Corp.) at 30°C for 15 min. Proteases were inactivated by the addition of an equal volume of 2×RIPA buffer (Lamb *et al.*, 1978) containing five proteinase inhibitors (pepstatin A, chymostatin, leupeptin, antipain each at 0.2 μg/ml and aprotinin at 0.025 TIU/ml). Proteins were immunoprecipitated with an HA specific antibody and the immune complex recovered by adsorption to protein A–Sepharose beads. Polypeptides were analyzed by SDS–PAGE on 15 or 10% polyacrylamide gels or 17.5% polyacrylamide gels containing 4 M urea, and the gels were processed for fluorography and autoradiography as described previously (Lamb and Choppin, 1976). Immunoblotting was performed by transferring polypeptides from a 15% SDS–polyacrylamide gel to a PVDF membrane (Immobilon-P membranes, Millipore) using a semi-dry transfer apparatus (Bio-Rad) according to

the manufacturers' instructions. The membrane was blocked with Blotto [5% dry milk in PBST (0.3% Tween 20 in PBS)] for 1 h. Following three successive washes with PBST, the blot was incubated for 60 min with goat polyclonal antiserum to A/Udorn/72 HA (SP31, a gift of Robert G.Webster) diluted 1/1000 in Blotto. After washing as above, the blot was then incubated for 60 min with peroxidase-conjugated rabbit anti-goat IgG (Cappel) diluted 1/1000 in Blotto. The blot was washed as before and stained with an ECL Western blot detection kit (Amersham) for 1 min and exposed to X-ray film.

Endoglycosidase treatment and labeling of virus-infected cell polypeptides in the presence of tunicamycin

Immunoprecipitation of virus-infected cell extracts with HA-specific antibody was performed as above. The immunoprecipitated proteins were eluted from protein A–Sepharose beads by boiling for 5 min in boiling buffer (0.4% SDS, 20 mM Na_2HPO_4, pH 8.0) and digested with 0.2 U of peptide *N*-glycosidase F in protease inhibitor buffer (40 mM Na_2HPO_4, pH 8.0, 20 mM EDTA, 1% NP40) overnight as described by Paterson and Lamb (1993). For tunicamycin treatment, infected CV-1 cells were incubated with 2 μg/ml of tunicamycin for 90 min after 4 h of infection, and medium was replaced with DME Met^-/Cys^- containing 2 μg/ml tunicamycin for 30 min. The cells were then labeled for 1 h with 100 μCi/ml Trans[^{35}S] label in the presence of tunicamycin and the monolayers were washed with PBS and lysed in RIPA buffer. Polypeptides were immunoprecipitated with HA-specific antibodies and analyzed on a 15% SDS–polyacrylamide gel.

Endo H digestion and cell surface trypsinization of HA

For endo H (endo-β-*N*-acetylglucosaminidase, ICN Biochemical) digestion, virus-infected cells at 5 h p.i. were incubated with DME Met^-/Cys^- for 30 min. Cells were labeled for 10 min with Trans[^{35}S] label (100 μCi/ml) in DME Met^-/Cys^-, incubated in chase medium for the indicated periods, and HA was immunoprecipitated. Immune complexes were digested with 1 mU of endo H for 18 h in citrate buffer as previously described (Paterson and Lamb, 1993). For cell surface trypsinization, infected CV-1 cells were labeled with Trans[^{35}S] label as above and incubated for various periods of chase. The monolayers were washed with PBS and incubated with 50 μg/ml TPCK–trypsin for 60 min at 4°C. The reaction was terminated by washing with 10% fetal bovine serum in PBS, cells were lysed in RIPA buffer containing proteinase inhibitors as described above, and HA was immunoprecipitated by using HA-specific polyclonal antisera (SP31).

Electron microscopy and Immunocytochemistry

The procedure for immunostaining purified virus was modified from that of Murti *et al.* (1985). Briefly, purified wild-type or $tail^-$ HA transfectant viruses were allowed to absorb onto parlodion-coated nickel grids for 30 s. Grids were floated on a drop of Tris-buffered saline (TBS; pH 7.4) for 5 min, after which they were blocked by floating on drops of 3% ovalbumin in TBS for 1 h. Grids were washed with TBS for 5 min and then incubated for 1 h with ascites fluid containing HA-specific monoclonal antibody D6/1 (a gift of Kathleen Coelingh) diluted 1/300 in 1% ovalbumin in TBS. Following three successive washes with TBS for 10 min each, samples were incubated for 1 h with goat anti-mouse antibody coupled to 10 nm gold particles diluted 1/10 in 1% ovalbumin in TBS. Colloidal gold and gold–antibody conjugates were prepared essentially as described by Slot and Geuze (1985). Grids were washed in TBS as above and finally stained with 2% phosphotungstic acid (pH 6.6). Prior to examination, a thin layer of carbon was evaporated onto the grids. Incubations were carried out at room temperature in a humidified chamber and all solutions were filtered before use.

For immunocytochemical analysis of virus budding, monolayers of MDCK cells were washed three times with PBS and infected (m.o.i. of 5) for 1 h at 37°C in an atmosphere containing 5% CO_2 with either wild-type or $tail^-$ HA transfectant virus. At 5 h p.i., cell monolayers were washed several times at 4°C with DME containing 10 mM HEPES (pH 7.3). All subsequent incubations were at 4°C unless otherwise stated. Cells were incubated for 1 h with ascites fluid containing the HA-specific monoclonal antibody D6/1 diluted 1/300 in DME plus 10 mM HEPES (pH 7.3), then washed with several changes of medium. Antibody binding was visualized by staining the monolayers for 1 h with goat anti-mouse antibody conjugated to 10 nm gold particles. After washing, cells were fixed for 2 h in 2% glutaraldehyde and post-fixed for 1 h in 1% osmium tetroxide, both in 0.1 M phosphate buffer, pH 7.2. In one experiment, infected cell cultures were returned to the 37°C incubator for 2 h following antibody staining but prior to fixation. Cells were dehydrated at room temperature through a graded ethanol series, ending with propylene oxide which also served to release the cell monolayers from the plastic tissue culture dishes. Cells were infiltrated and embedded in epoxy resin, 60–80 nm sections were collected on parlodion-coated copper grids, and stained with uranyl acetate and lead citrate.

Budding virus was quantified by taking random electron micrographs of infected cells. Prints were enlarged to a final magnification of 20 000 and were randomly overlaid with a grid corresponding to a 1 μm lattice. Membrane length was measured by counting intersections with the grid, and budding viruses, identified by their characteristic morphology and heavy staining with HA-specific monoclonal antibody, were counted. For both wild-type and $tail^-$ HA transfectant infected cells three separate infections were quantified, and virus was counted over a membrane length of ~200 μm for each infection.

Acknowledgements

We thank Mark Krystal and Peter Palese both for advice and for making available reagents that helped establish the reverse genetics system in our laboratory, and we thank John K.Rose for discussions concerning virus assembly. H.J. is an associate and R.A.L. is an investigator of the Howard Hughes Medical Institute. This research was supported in part by Public Health Service research grant AI-20201 from the National Institute of Allergy and Infectious Diseases.

References

Ausubel,F.M., Brent,R., Kingston,R.E., Moore,D.D., Seidman,J.G., Smith,J.A. and Struhl,K. (eds) (1994) *Current Protocols in Molecular Biology*. Wiley and Sons, New York, Vols 1 and 2.

Balch,W.E., McCaffery,J.M., Plutner,H. and Farquhar,M.G. (1994) *Cell*, **76**, 841–852.

Bilsel,P., Castrucci,M.R. and Kawaoka,Y.(1993) *J. Virol.*, **67**, 6762–6767.

Bron,R., Kendal,A.P., Klenk,H.-D. and Wilschut,J. (1993) *Virology*, **195**, 808–811.

Chakrabarti,L., Emerman,M., Tiollais,P. and Sonigo,P. (1989) *J. Virol.*, **63**, 4395–4403.

Collier,N.C., Knox,K. and Schlesinger,M.J.(1991) *Virology*, **183**, 769–772.

Compans,R.W. and Choppin,P.W. (1975) In Fraenkel-Conrat,H. and Wagner,R.R. (eds), *Comprehensive Virology*. Plenum, New York, Vol. IV, pp. 179–252.

Doyle,C., Roth,M.G., Sambrook,J. and Gething,M.-J. (1985) *J. Cell Biol.*, **100**, 704–714.

Doyle,C., Sambrook,J. and Gething,M.-J. (1986) *J. Cell Biol.*, **103**, 1193–1204.

Dubois-Dalcq,M., Holmes,K.V. and Rentier,B. (1984) *Assembly of Enveloped RNA Viruses*. Springer-Verlag, New York.

Enami,M. and Palese,P. (1991) *J. Virol.*, **65**, 2711–2713.

Gaedigk-Nitschko,K. and Schlesinger,M.J. (1991) *Virology*, **183**, 206–214.

Hirst,G.K. (1942) *J. Exp. Med.*, **75**, 47–64.

Kemble,G.W., Danieli,T. and White,J.M.(1994) *Cell*, **76**, 383–391.

Lamb,R.A. (1989) In Krug,R.M. (ed.), *The Influenza Viruses*. Plenum Publishing Corp., New York, pp. 1–87.

Lamb,R.A. and Choppin,P.W.(1976) *Virology*, **74**, 504–519.

Lamb,R.A., Etkind,P.R. and Choppin,P.W. (1978) *Virology*, **91**, 60–78.

Lamb,R.A., Zebedee,S.L and Richardson,C.D. (1985) *Cell*, **40**, 627–633.

Li,S., Schulman,J.L., Moran,T., Bona,C. and Palese,P. (1992) *J. Virol.*, **66**, 399–404.

Liu,C. and Air,G.M. (1993) *Virology*, **194**, 403–407.

Lopez,S., Yao,J.-S., Kuhn,R.J., Strauss,E.G. and Strauss,J.H. (1994) *J. Virol.*, **68**, 1316–1323.

Luytjes,W., Krystal,M., Enami,M., Parvin,J.D. and Palese,P. (1989) *Cell*, **59**, 1107–1113.

Marsh,M. and Helenius,A. (1989) *Adv. Virus Res.*, **36**, 107–151.

Metsikko,K. and Simons,K. (1986) *EMBO J.*, **5**, 1913–1920.

Murti,K.G., Portner,A., Troughton,K. and Deshpande,K. (1985) *J. Electron. Microsc. Tech.*, **2**, 139–146.

Naeve,C.W. and Williams,D. (1990) *EMBO J.*, **9**, 3857–3866.

Naim,H.Y., Amarneh,B., Ktistakis,N.T. and Roth,M.G. (1992) *J. Virol.*, **66**, 7585–7588.

Naim,H.Y. and Roth,M.G. (1993) *J. Virol.*, **67**, 4831–4841.

Nobusawa,E., Aoyama,T., Kato,H., Suzuki,Y., Tateno,Y. and Nakajima,K. (1991) *Virology*, **182**, 475–485.

Palese,P., Tobita,K., Ueda,M. and Compans,R.W. (1974) *Virology*, **61**, 397–410.
Parvin,J.D., Palese,P., Honda,A., Ishihama,A. and Krystal,M. (1989) *J. Virol.*, **63**, 5142–5152.
Paterson,R.G. and Lamb,R.A.(1993) In Davidson,A. and Elliott,R.M. (eds), *Molecular Virology: A Practical Approach*. IRL at Oxford University Press, Oxford, pp. 35–73.
Pattnaik,A.K., Brown,D.J. and Nayak,D.P. (1986) *J. Virol.*, **60**, 994–1001.
Perez,L.G., Davis,G.L. and Hunter,E. (1987) *J. Virol.*, **61**, 2981–2988.
Pinto,L.H., Holsinger,L.J. and Lamb,R.A. (1992) *Cell*, **69**, 517–528.
Sanger,F., Nicklin,S. and Coulson,A.R. (1977) *Proc. Natl Acad. Sci. USA*, **74**, 5463–5467.
Simpson,D.A. and Lamb,R.A. (1992) *J. Virol.*, **66**, 790–803.
Simons,K. and Garoff,H. (1980) *J. Gen. Virol.*, **50**, 1–21.
Slot,J.W. and Geuze,H.J. (1985) *Eur. J. Cell Biol.*, **38**, 87–93.
Steinhauer,D.A., Wharton,S.A., Wiley,D.C. and Skehel,J.J. (1991) *Virology*, **184**, 445–448.
Viet,M., Kretzschmar,E., Kuroda,K., Garten,W., Schmidt,M.F.G., Klenk,H.-D. and Rott,R. (1991) *J. Virol.*, **65**, 2491–2500.
Wang,C., Takeuchi,K., Pinto,L.H. and Lamb,R.A. (1993) *J. Virol.*, **67**, 5585–5594.
Whitt,M.A., Chong,L. and Rose,J.K. (1989) *J. Virol.*, **63**, 3569–3578.
Weis,W., Brown,J.H., Cusack,S., Paulson,J.C., Skehel,J.J. and Wiley,D.C. (1988) *Nature*, **333**, 426–431.
Winship,P.R. (1989) *Nucleic Acids Res.*, **17**, 1266.
Zebedee,S.L., Richardson,C.D. and Lamb, R.A. (1985) *J. Virol.*, **56**, 502–511.
Zebedee,S.L. and Lamb,R.A. (1988) *J. Virol.*, **62**, 2762–2772.
Zebedee,S.L. and Lamb,R.A. (1989) *Proc. Natl Acad. Sci. USA*, **86**, 1061–1065.

Received on July 21, 1994; revised on September 1, 1994